Dalton Transactions

Accepted Manuscript

ROYAL SOCIETY OF CHEMISTRY

www.rsc.org/dalton

Dalton Transactions

Dynamic Article Links ►

Cite this: DOI: 10.1039/c0xx00000x

www.rsc.org/xxxxxx

ARTICLE TYPE

Artificial Synthetic $Mn^{IV}Ca$-oxido Complexes Mimic the Oxygen-Evolving Complex in Photosystem II

Changhui Chen[a,b], Chunxi Zhang*[a], Hongxing Dong*[b], Jingquan Zhao[a]

Received (in XXX, XXX) Xth XXXXXXXXX 20XX, Accepted Xth XXXXXXXXX 20XX

DOI: 10.1039/b000000x

A novel family of heteronuclear $Mn^{IV}Ca$-oxido complexes containing $Mn^{IV}Ca$-oxido cuboidal moieties and reactive water molecules on Ca^{2+} have been synthesized and characterized to mimic the oxygen-evolving complex (OEC) of photosystem II (PSII) in nature.

The oxygen-evolving complex (OEC) within photosystem II (PSII) of plants, algae and cyanobacteria is a unique catalyst for water oxidation in nature, which serves as a blueprint for the development of artificial catalysts for water splitting to generate hydrogen fuel as renewable energy source[1-6]. The structure of the OEC and the mechanism of water-splitting reaction have abstracted extensively attentions in the last two decades. Recently, the structure of the OEC has been revealed by the X-ray crystal structure of PSII [7, 8]. In the core of the OEC, one Ca^{2+} ion is incorporated into the Mn_4-cluster through two μ_3-O^{2-} and one μ_4-O^{2-} oxido moieties to form a unique $[Mn_4CaO_5]$ catalytic site as shown in **Figure 1**. The peripheral ligands of the OEC are mainly consisted of carboxylate groups of amino acids from D_1 and CP_{43} proteins[7, 8]. Four water molecules were found to coordinate to OEC with two (W1, W2) associated to Mn4 and the other two (W3, W4) on Ca^{2+}[8]. The turnover of the OEC for water-splitting involves five different S-states (S_n, n = 0 ~ 4). Due to the involvment of a large protein matrix and the structural complexity and uncertainty of the OEC in higher S-states[9-15], the mechanism of O–O bond formation[16-21] and functional roles of Ca^{2+}[22-25] remains under debate. To deepen understanding the structure of the OEC and the mechanism of water-splitting reaction in nature, it is highly desirable to synthesize structurally well defined small-molecule models to mimic the OEC in laboratory.

To data, although many Mn complexes[3, 6, 26-28] and MnCa complexes[29-38] have been reported in literatures, it is of a great challenge for chemists to synthesize a structural model with similar MnCa-oxido core structure, peripheral carboxylate ligands and the ligation of four water molecules as observed in the OEC of PSII at the same time.

We herein report the synthesis and characterization of a novel family of heteronuclear $Mn^{IV}Ca$-oxido complexes containing MnCaO cuboidal moieties and reactive water molecules on Ca^{2+} to mimic the OEC in PSII.

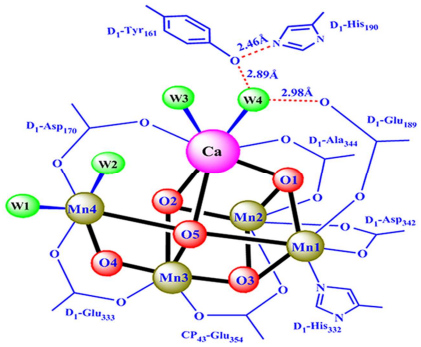

Figure 1 Scheme for the structure of the OEC in PSII

Complex **A** was synthesized in a reaction of $Bu^n_4NMnO_4$, $Mn(ClO_4)_2•(H_2O)_6$ and $Ca(CH_3CO_2)_2$ with a molar ratio of 4 : 1 : 1 in boiling acetonitrile with the presence of an excess of pivalic acid, which was similar to the method developed recently for the synthesis of the $[Mn_3SrO_4]_2O$ complex[28]. The crystal of **A**, $[Mn^{IV}_6Ca_2O_9(Bu^tCO_2)_{10}(H_2O)_4]•(Bu^tCO_2H)_5$, as obtained as dark-brown crystals formed after mixing of 10 % hexane (v/v). Complex **B**, $[Mn^{IV}_6Ca_2O_9(Bu^tCO_2)_{10}(H_2O)_3(CH_3CO_2C_2H_5)]•(Bu^tCO_2H)_3•(CH_3CO_2C_2H_5)$, was obtained from the solution of **A** in ethyl acetate. Complex **C**, $[Mn^{IV}_6Ca_2O_9(Bu^tCO_2)_{11}]•[Mn^{III}_3O(Bu^tCO_2)_6(py)_3]•(CH_3CN)_3$, was formed as dark-brown crystal isolated from the acetonitrile solution of **A** in the presence of ~2 % pyridine. For details of preparations, see Supporting Information.

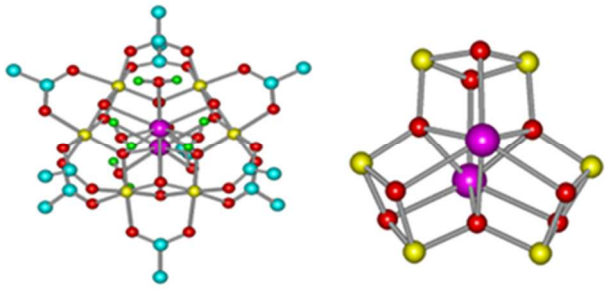

Figure 2 Whole structure (left) and $[Mn_6Ca_2O_9]$ core (right) of **A**. For clarity, all pivalic CH_3 groups are omitted, and all unbinding pivalic acids are omitted as well. Mn, Ca, O, C, and H atoms are shown in yellow, violet, red, cyan and green, respectively.

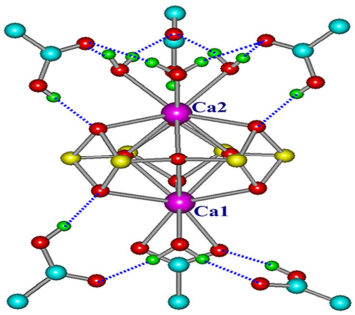

Figure 3 The H-bond network in **A**. The dashed-lines display the H-bond interactions. Other illustrations are the same as those in **Figure 2**.

The core of **A** (**Figure 2**) contains three $[Mn_2Ca_2O_4]$ distorted cubanes sharing a trigonal-bipyramidal $[Ca_2O_3]$ unit in the center, which is significantly different from our previous $[Mn^{IV}{}_6Sr_2O_9]$ complex containing two $[Mn_3SrO_4]$ cubanes linked by one μ_2-O^{2-} anion[28]. Two Ca^{2+} ions are connected to Mn ions by three μ_3-O^{2-} and three μ_4-O^{2-} anions, and completely coordinated by carboxylate and H_2O molecules. The coordinated H_2O molecules further interact with five uncoordinated pivalic acid molecules through H-bonds network (**Figure 3**). In the $[Mn_2Ca_2O_4]$ cubane, the distances of Mn…Mn and Mn...Ca are 2.71 Å and 3.46 Å, respectively. The bond lengths of Mn–oxido (1.80–1.86 Å), Ca^{2+}–oxido (2.42 ~ 2.64 Å) and Ca^{2+}–O_{water} (2.38 ~ 2.44 Å) are similar to those observed in reported multinuclear Mn oxido complexes[31, 34, 38] and the OEC in PSII[8]. Bond-valence sum (BVS) calculations[39] shows that all bridged oxygen atoms are in deprotonated state and all Mn ions are in +4 oxidation state(**Table 1 and Table S1**). The assignment of +4 valences for all six Mn ions are also supported by the values (2.8 ~ 2.9) of the Mulliken atomic spin densities obtained by density functional theory (DFT) calculation (**Table 1**).

Complex **A** dispalys an irreversible oxidation at + 0.85 V *vs*. NHE as revealed by the cyclic voltammograms measurement (**Figure 4**), which was almost the same as the value of +0.8 V to +0.9 V *vs*. NHE observed for the OEC in PSII[40]. We noted that this high redox potential was not observed in previous $[Mn^{IV}{}_3Ca]$ complexes[34] primarily coordinated by dipyridylalkoxide, but it is close to the 0.9 V *vs*. NHE observed in the $[Mn^{IV}{}_3SrO_4]_2O$ complex primarily coordinated by multiple carboxylate groups[28] similar as that of **A**. Because the valence of all six Mn ions in **A** is +4, we tentatively assign the oxidation peak at 0.85 V *vs*. NHE (**Figure 4)** to the formation of Mn^V species. Generally, Mn^V would be highly reactive, and it is difficult to be trapped[41, 42]. However, the presence of one Ca^{2+} has been shown to stabilize the high oxidation state of Mn ions in various MnCa-oxido complexes[34, 38]. Accordingly, the two Ca^{2+} ions in **A** may contribute significantly to stabilize the high reactive species, Mn^V, as well, similar to that in previous reports[34, 38]. The Mn^V species was proposed to be involved during the turnover of the OEC in PSII in literatures[1, 2, 27]. Therefore, the electrochemical properties of the model complex reported here may provide chemical insights into understanding the mechanism of water splitting in PSII.

Table 1. The oxidation states of all Mn ions in **A** from BVS calculation and DFT calculation

Atoms	BVS	Mulliken atomic spin densities	Assignment
Mn1	4.080	2.887	Mn^{IV}
Mn2	4.161	2.817	Mn^{IV}
Mn3	4.145	2.858	Mn^{IV}
Mn4	4.124	2.889	Mn^{IV}
Mn5	4.114	2.881	Mn^{IV}
Mn6	4.121	2.877	Mn^{IV}

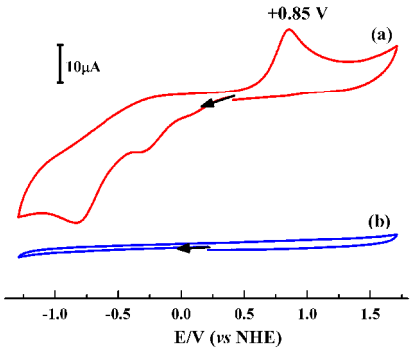

Figure 4 Cyclic voltammogram (CV) of **A** in 1,2-dichloroethane. (a) With 1mM of **A**; (b) Without **A**. Potentials are referenced to NHE. Scan rate: 100 mV s^{-1}, arrows display the scan direction.

The core fraction and the coordinated H_2O molcules of **A** show striking structural similarities to that of the OEC in PSII (**Figure 5**). To our knowledge, this is the first time to obtain an artificial Mn^{IV}Ca-oxido complex with $[Ca(H_2O)n]$ (n =1 or 3) unit incorporated to the multinuclear Mn^{IV} cluster through the μ_3-O^{2-} and μ_4-O^{2-} bridges as observed in the OEC of PSII. Therefore, complex **A** might be a good chemical model to investigate the functional roles of the water molecules on Ca^{2+} in the OEC of PSII.

We have found that the $[Mn^{IV}{}_6Ca_2O_9]$ core structure was stable in various solvents (e.g. ethyl acetate, toluene, and hexane), which is consistent with the finding that the presence of Ca^{2+} ion could significantly stabilize the high oxidation states Mn ions[34, 38]. On the other hand, the binding water molecules on Ca^{2+} were reactive under various experimental conditions, as demonstrated in the structures of **B** and **C**.

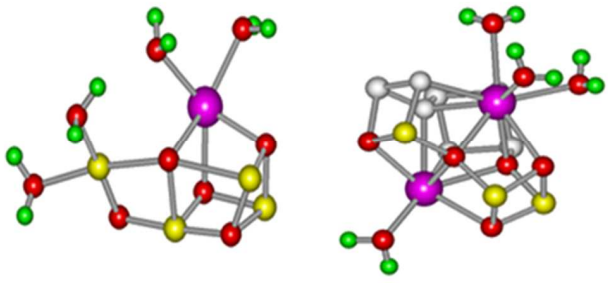

Figure 5 Structure of the core and coordinated water molecules in the OEC (left) and **A** (right). For clarity, only the $Mn_3Ca_2O_5(H_2O)_4$ fraction of **A** similar to that of the OEC is shown in color, and the left fraction is shown in light grey. Other illustrations are the same as those in **Figure 2**.

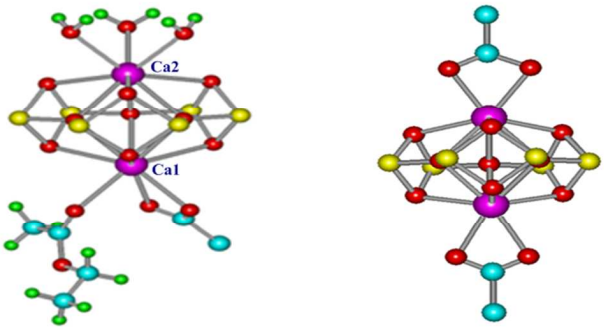

Figure 6 Structures of the $[Mn_6Ca_2O_9]$ core in **B** (left) and **C** (right)**.** The two carboxylate groups on Ca^{2+} ions in **C** are in symmetry-imposed disorder in crystal structural data, and only one pattern was shown for clarity. Other illustrations are the same as those in **Figure 2**.

Table 2. Selected bond lengths (Å) in **A**, **B** and **C.**

Bond	A	B	C
Mn–Mn	2.704-2.718	2.702-2.709	2.683
Mn–Ca	3.445-3.522	3.444-3.531	3.434-3.476
μ_3-O^{2-}–Mn	1.811-1.856	1.818-1.856	1.816-1.827
μ_4-O^{2-}–Mn	1.799-1.816	1.808-1.818	1.812-1.831
μ_3-O^{2-}–Ca	2.576-2.641	2.583-2.654	2.579-2.615
μ_4-O^{2-}–Ca	2.433-2.520	2.426-2.507	2.422-2.439
Mn–O_{piv}	1.931-1.980	1.946-1.979	1.956-1.992

Table 2 shows the selected bond lengths of the $[Mn_6Ca_2O_9(Bu^tCO_2)_9]$ unit in complexes **A**, **B** and **C**. The distances of Mn–Mn (~ 2.70 Å), Mn–Ca (3.4 ~ 3.5 Å), μ_3-O^{2-}–Mn (1.81 ~ 1.86 Å), μ_4-O^{2-}–Mn (1.80 ~ 1.83 Å) and Mn–O_{piv} (1.93 ~ 2.00 Å) in three complexes are very similar, clearly indicating that the basic structure of the $[Mn_6Ca_2O_9(Bu^tCO_2)_9]$ unit was undisturbed in these complexes.

In complex **B** (**Figure 6** left), one H_2O on Ca1 was replaced by an ethyl acetate molecule; while the binding of the three H_2O on Ca2 were undisturbed. It is likely that the ligation of the three H_2O molecules on Ca2 was stabilized by a crown-shaped H-bond network with peripheral pivalic acid molecules (see **Figure 3**). In contrary, all four H_2O molecules on both Ca^{2+} ions were replaced by carboxylate groups in **C** (**Figure 6** right). It is likely that the strength of those H-bonds in **A** and **B** (**Figure 3** and **Figure S2**) could be significantly disturbed in the polar solvent[43] (*e.g.* acetonitrile), resulting in the replacement of all H_2O molecules in **C**.

Obviously, the H_2O molecules on Ca^{2+} ions are exchangeable, and can be replaced by the oxygen atom of carbonyl or carboxylate groups under various conditions, depending on the H-bond interactions with peripheral environments. The presence of the well-ordered H-bonds could significantly contribute to stabilize the binding of water molecules on Ca^{2+}. These results provide important clues into understanding the reactivity of two H_2O molecules on Ca^{2+} in the OEC of PSII.

One key issue to understand the mechanism of the O–O bond formation in PSII is whether these H_2O molecules (W3, W4) on Ca^{2+} revealed by X-ray structure could play a role as substrate [5, 22-24, 44-46]. According to our observations in complexes **A**, **B** and **C**, one could expect that the binding affinity of W4 water molecule might be higher than that of W3, due to the presence of a well-ordered H-bond interactions between the former and D_1-Tyr_{161} and D_1-Glu_{189} (**Figure 1**), but not the latter. In addition, the nearby residue of D_1-Glu_{189} may be able to coordinate to the Ca^{2+} and replace the W3 water molecule through its free carboxylate oxygen atom (**Figure 1** and **Figure 7**), similar to the carboxylate or carbonyl groups on the Ca^{2+} in **B** and **C**. If this is the case, one would expect that the W4 water molecule should not be a substrate, instead, the W3 might be able to be involved more directly to the formation of O–O bond at the higher S-state of the OEC. Consequently, with the participating of the nearby D_1-Glu_{189}, one possible mechanism for the O–O bond formation could occur between the W2 and W3 water molcules on the OEC (shown in **Figure 7**). This proposal is consistent with previous suggestions[8, 16, 22-24]. However, we should point out that there are other possiblities for the formation of O–O bond without involving the W4 water molecule as substrate [16-18, 21, 46]. For example, based on theoretical calculation[17] and high filed electron parapmagnatic resonance (HFEPR) study[21] on the S_3 state OEC, it has been suggested that the O5 atom could sever as a source of oxygen atoms for the formation of O-O bond in the higher S-states (*e.g.* S_3, S_4) of the OEC[17, 21].

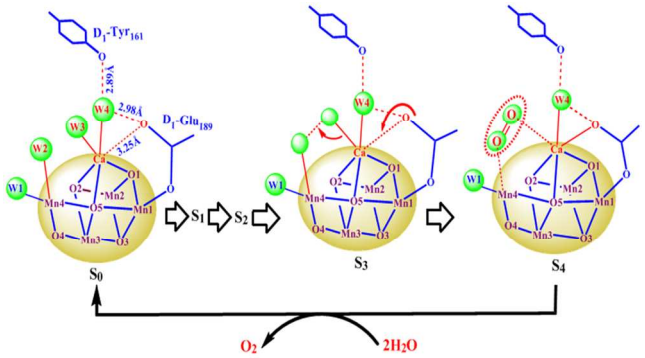

Figure 7 One possible mechanism for the O—O bond formation during water oxidation in PSII. Dashed lines display H-bond or weak interactions.

In summary, three heteronuclear $Mn^{IV}Ca$-oxido complexes have been synthesized and characterized, which display remarkable structural similarities to the OEC in PSII, in respects of the peripheral ligands, the $Mn_2Ca_2O_4$ cuboidal moiety, especially, the coordination of reactive water molecules on Ca^{2+}. The water molecules on Ca^{2+} ions in these artificial complexes can be replaced by carbonyl or carboxylate groups, depending on the H-bond interactions with peripheral environments. These results provide new insight into the understanding of the structural and functional roles of the Ca^{2+} in the OEC of PSII in nature.

This work was supported by the National Natural Science Foundation of China (No. 31070216, 91427303), the Chinese Academy of Sciences (KJCX2-YW-W25) and the Fundamental Research Funds for the Central Universities of China (No. HEUCFT1009, HEUCF201403008).

Notes and references

[a] *Laboratory of Photochemistry, Institute of Chemistry, Chinese Academy of Sciences, Beijing 100190, China. Fax: 86-10-82617315; Tel: 86-10-82617053; E-mail: chunxizhang@iccas.ac.cn*

[b] *Polymer Materials Research Center, Key Laboratory of Superlight Materials & Surface Technology of Ministry of Education, College of Materials Science and Chemical Engineering, Harbin Engineering*

University, Harbin 150001, China, Tel: 86-451-82568191; E-mail: dhongxing@hrbeu.edu.cn

† Electronic Supplementary Information (ESI) available: [Experimental section, BVS calculation, computational details, X-ray structure information, UV-vis absorption spectrum]. See DOI: 10.1039/b000000x/

‡Elemental analysis (%) calcd. for **A** ($C_{81}H_{162}Ca_2Mn_6O_{43}$): C, 43.55; H, 7.31; found: C, 43.30; H, 7.35.Crystal structure data for complex **A** $[Mn_6Ca_2O_9(Bu^tCO_2)_{10}(H_2O)_4]\bullet(Bu^tCO_2H)_5$: $C_{75}H_{148}Ca_2Mn_6O_{43}$, M = 2147.73 g/mol , black lump crystal, triclinic, P-1, a = 14.878(3) Å, b = 15.831(3) Å, c = 26.221(5) Å, α = 93.680(2) °, β = 97.730(3) °, γ = 112.599(3) °, V = 5604(2) Å^3, 42124 reflections collected; 1210 parameters were refined in the final cycle of refinement using 19641 reflections ($I > 2\sigma(I)$); $R1$ = 0.1148, $wR2$ = 0.2570 (based on F^2 and all data).

Elemental analysis (%) calcd. for **B** ($C_{69}H_{134}Ca_2Mn_6O_{40}$): C, 41.16, H, 6.71 %. found: C, 40.97, H, 6.70. Crystal structure data for complex **B** $[Mn^{IV}{}_6Ca_2O_9(Bu^tCO_2)_{10}(H_2O)_3(CH_3CO_2C_2H_5)]\bullet(Bu^tCO_2H)_3\bullet(CH_3CO_2C_2H_5)$: $C_{73}H_{142}Ca_2Mn_6O_{42}$, M = 2101.66 g/mol, black lump crystal, monoclinic, $I2/a$, a = 26.486(5) Å, b = 30.822(6) Å, c = 26.925(4) Å, α = 90.0 °, β = 109.39(2)°, γ = 90.0 °, V = 20734(7) Å^3, 70319 reflections collected; 1183 parameters were refined in the final cycle of refinement using 23662 reflections ($I > 2\sigma(I)$); $R1$ = 0.1297, $wR2$ = 0.1914 (based on F^2 and all data).

Elemental analysis (%) calcd. for **C** ($C_{100}H_{168}Ca_2Mn_9N_3O_{44}$): C, 44.63; H, 6.29; N, 1.56. found: C, 44.60; H, 6.42; N, 1.83. Crystal structure data for complex **C** $[Mn_6Ca_2O_9(Bu^tCO_2)_{11}Mn_3O(Bu^tCO_2)_6(py)_3]\bullet(CH_3CN)_3$: $C_{106}H_{177}Ca_2Mn_9N_6O_{44}$, M = 2814.14 g/mol,, black triquetrous crystal, cubic, $P2_13$, a = 24.4452(4) Å, b = 24.4452(4) Å, c = 24.4452(4) Å, α = 90.0 °, β = 90.0 °, γ = 90.0 °, V = 14607.7(7) Å^3, 18874 reflections collected; 544 parameters were refined in the final cycle of refinement using 10502 reflections ($I > 2\sigma(I)$); $R1$ = 0.1187, $wR2$ = 0.2423 (based on F^2 and all data).

All crystallographic data were stored in the Cambridge Crystallographic Data Centre with CCDC codes, 1039345, 1039346 and 1039344 for complex **A**, **B** and **C**, respectively.

1. J. P. McEvoy and G. W. Brudvig, *Chem. Rev.*, 2006, **106**, 4455-4483.
2. J. Barber, *Chem. Soc. Rev.*, 2009, **38**, 185-196.
3. G. C. Dismukes, R. Brimblecombe, G. A. N. Felton, R. S. Pryadun, J. E. Sheats, L. Spiccia and G. F. Swiegers, *Acc. Chem. Res.*, 2009, **42**, 1935-1943.
4. H. Dau, I. Zaharieva and M. Haumann, *Cur. Opin. Chem. Biol.*, 2012, **16**, 3-10.
5. J. Yano and V. Yachandra, *Chem. Rev.*, 2014, **114**, 4175-4205.
6. M. D. Kärkäs, E. V. Johnston, O. Verho and B. Åkermark, *Acc. Chem. Res.*, 2014, **47**, 100-111.
7. K. N. Ferreira, T. M. Iverson, K. Maghlaoui, J. Barber and S. Iwata, *Science*, 2004, **303**, 1831-1838.
8. Y. Umena, K. Kawakami, J. R. Shen and N. Kamiya, *Nature*, 2011, **473**, 55-60.
9. J. Yano, J. Kern, K. D. Irrgang, M. J. Latimer, U. Bergmann, P. Glatzel, Y. Pushkar, J. Biesiadka, B. Loll, K. Sauer, J. Messinger, A. Zouni and V. K. Yachandra, *Proc. Natl. Acad. Sci. USA*, 2005, **102**, 12047-12052.
10. M. Grabolle, M. Haumann, C. Müller, P. Liebisch and H. Dau, *J. Biol. Chem.*, 2006, **281**, 4580-4588.
11. S. Luber, I. Rivalta, Y. Umena, K. Kawakami, J. R. Shen, N. Kamiya, G. W. Brudvig and V. S. Batista, *Biochemistry*, 2011, **50**, 6308-6311.
12. A. Galstyan, A. Robertazzi and E. W. Knapp, *J. Am. Chem. Soc.*, 2012, **134**, 7442-7449.
13. A. Grundmeier and H. Dau, *Biochim. Biophys. Acta*, 2012, **1817**, 88-105.
14. C. Glöckner, J. Kern, M. Broser, A. Zouni, V. Yachandra and J. Yano, *J. Biol. Chem.*, 2013, **288**, 22607-22620.
15. Y. Wang, C. Zhang, L. Wang and J. Zhao, *Chin. Sci. Bull.*, 2013, **58**, 3213-3216.
16. H. Isobe, M. Shoji, S. Yamanaka, Y. Umena, K. Kawakami, N. Kamiya, J. R. Shen and K. Yamaguchi, *Dalton Trans.*, 2012, **41**, 13727-13740.
17. P. E. M. Siegbahn, *Biochim. Biophys. Acta*, 2013, **1827**, 1003-1019.
18. M. Kusunoki, *J. Photochem. Photobiol. B*, 2011, **104**, 100-110.
19. D. A. Pantazis, W. Ames, N. Cox, W. Lubitz and F. Neese, *Angew. Chem. Int. Ed.*, 2012, **51**, 9935-9940.
20. N. Cox, D. A. Pantazis, F. Neese and W. Lubitz, *Acc. Chem. Res.*, 2013, **46**, 1588-1596.
21. N. Cox, M. Retegan, F. Neese, D. A. Pantazis, A. Boussac and W. Lubitz, *Science*, 2014, **345**, 804-808.
22. V. L. Pecoraro, M. J. Baldwin, M. T. Caudle, W. Y. Hsieh and N. A. Law, *Pure Appl. Chem.*, 1998, **70**, 925-929.
23. J. P. McEvoy and G. W. Brudvig, *Phys. Chem. Chem. Phys.*, 2004, **6**, 4754-4763.
24. M. Lundberg and P. E. M. Siegbahn, *Phys. Chem. Chem. Phys.*, 2004, **6**, 4772-4780.
25. C. F. Yocum, *Coord. Chem. Rev.*, 2008, **252**, 296-305.
26. S. Mukhopadhyay, S. K. Mandal, S. Bhaduri and W. H. Armstrong, *Chem. Rev.*, 2004, **104**, 3981-4026.
27. C. S. Mullins and V. L. Pecoraro, *Coord. Chem. Rev.*, 2008, **252**, 416-443.
28. C. Chen, C. Zhang, H. Dong and J. Zhao, *Chem. Commun.*, 2014, **50**, 9263-9265.
29. A. Mishra, W. Wernsdorfer, K. A. Abboud and G. Christou, *Chem. Commun.*, 2005, 54-56.
30. I. J. Hewitt, J. K. Tang, N. T. Madhu, R. Clerac, G. Buth, C. E. Anson and A. K. Powell, *Chem. Commun.*, 2006, 2650-2652.
31. A. Mishra, J. Yano, Y. Pushkar, V. K. Yachandra, K. A. Abboud and G. Christou, *Chem. Commun.*, 2007, 1538-1540.
32. L. B. Jerzykiewicz, J. Utko, M. Duczmal and P. Sobota, *Dalton Trans.*, 2007, 825-826.
33. E. S. Koumousi, S. Mukherjee, C. M. Beavers, S. J. Teat, G. Christou and T. C. Stamatatos, *Chem. Commun.*, 2011, **47**, 11128-11130.
34. J. S. Kanady, E. Y. Tsui, M. W. Day and T. Agapie, *Science*, 2011, **333**, 733-736.
35. S. Nayak, H. P. Nayek, S. Dehnen, A. K. Powell and J. Reedijk, *Dalton Trans.*, 2011, **40**, 2699-2702.
36. Y. J. Park, J. W. Ziller and A. S. Borovik, *J. Am. Chem. Soc.*, 2011, **133**, 9258-9261.
37. S. Mukherjee, J. A. Stull, J. Yano, T. C. Stamatatos, K. Pringouri, T. A. Stich, K. A. Abboud, R. D. Britt, V. K. Yachandra and G. Christou, *Proc. Natl. Acad. Sci. USA*, 2012, **109**, 2257-2262.
38. E. Y. Tsui, R. Tran, J. Yano and T. Agapie, *Nat. Chem.*, 2013, **5**, 293-299.
39. W. Liu and H. H. Thorp, *Inorg. Chem.*, 1993, **32**, 4102-4105.
40. H. Dau and I. Zaharieva, *Acc. Chem. Res.*, 2009, **42**, 1861-1870.
41. Y. Gao, T. Åkermark, J. Liu, L. Sun and B. Åkermark, *J. Am. Chem. Soc.*, 2009, **131**, 8726-8727.
42. Y. Shimazaki, T. Nagano, H. Takesue, B. H. Ye, F. Tani and Y. Naruta, *Angew Chem., Int. Ed. Engl*, 2004, **43**, 98-100.
43. P. Gilli, L. Pretto, V. Bertolasi and G. Gilli, *Acc. Chem. Res*, 2009, **42**, 33-44.
44. C. W. Hoganson and G. T. Babcock, *Science*, 1997, **277**, 1953-1956.
45. C. Zhang, *Biochim. Biophys. Acta*, 2007, **1767**, 493-499.
46. N. Cox and J. Messinger, *Biochim. Biophys. Acta*, 2013, **1827**, 1020-1030.

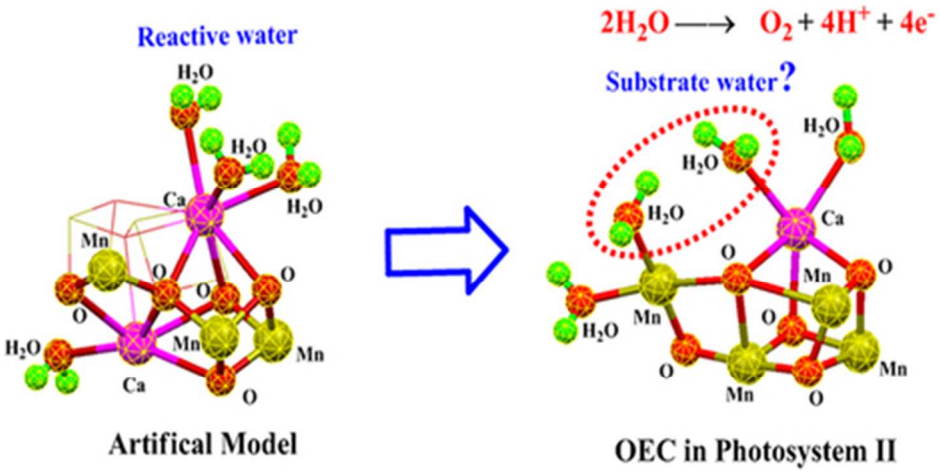

39x19mm (300 x 300 DPI)

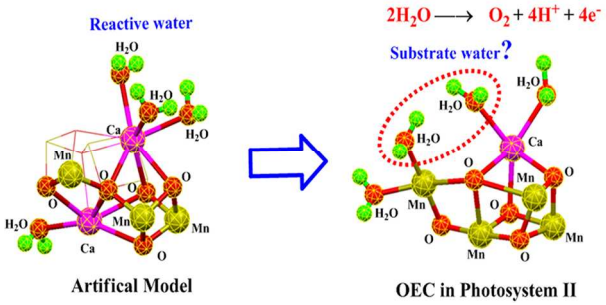

Highlight: Artificial synthetic $Mn^{IV}Ca$-oxido complexes containing reactive water molecules have been synthesized to mimic the oxygen-evolving center in photosystem II.